Specific Hepatic Sphingolipids Relate to Insulin Resistance, Oxidative Stress, and Inflammation in Nonalcoholic Steatohepatitis

Maria Apostolopoulou,[1,2,3] Ruth Gordillo,[4] Chrysi Koliaki,[2,3] Sofia Gancheva,[1,2,3] Tomas Jelenik,[2,3] Elisabetta De Filippo,[2,3] Christian Herder,[2,3] Daniel Markgraf,[2,3] Frank Jankowiak,[5] Irene Esposito,[5] Matthias Schlensak,[6] Philipp E. Scherer,[4] and Michael Roden[1,2,3]

Diabetes Care 2018;41:1235–1243 | https://doi.org/10.2337/dc17-1318

OBJECTIVE

Insulin resistance and nonalcoholic fatty liver disease have been linked to several lipid metabolites in animals, but their role in humans remains unclear. This study examined the relationship of sphingolipids with hepatic and peripheral metabolism in 21 insulin-resistant obese patients without (NAFL−) or with (NAFL+) nonalcoholic fatty liver and nonalcoholic steatohepatitis (NASH) and 7 healthy lean individuals undergoing tissue biopsies during bariatric or elective abdominal surgery.

RESEARCH DESIGN AND METHODS

Hyperinsulinemic-euglycemic clamps with D-[6,6-$^2H_2$]glucose were performed to quantify tissue-specific insulin sensitivity. Hepatic oxidative capacity, lipid peroxidation, and the phosphorylated-to-total c-Jun N-terminal kinase (pJNK-to-tJNK) ratio were measured to assess mitochondrial function, oxidative stress, and inflammatory activity.

RESULTS

Hepatic total ceramides were higher by 50% and 33% in NASH compared with NAFL+ and NAFL−, respectively. Only in NASH were hepatic dihydroceramides (16:0, 22:0, and 24:1) and lactosylceramides increased. Serum total ceramides and dihydroceramides (hepatic dihydroceramides 22:0 and 24:1) correlated negatively with whole-body but not with hepatic insulin sensitivity. Hepatic maximal respiration related positively to serum lactosylceramide subspecies, hepatic sphinganine, and lactosylceramide 14:0. Liver lipid peroxides (total ceramides, sphingomyelin 22:0) and the pJNK-to-tJNK ratio (ceramide 24:0; hexosylceramides 22:0, 24:0, and 24:1) all positively correlated with the respective hepatic sphingolipids.

CONCLUSIONS

Sphingolipid species are not only increased in insulin-resistant humans with NASH but also correlate with hepatic oxidative stress and inflammation, suggesting that these lipids may play a role during progression of simple steatosis to NASH in humans.

Obesity, insulin resistance, and type 2 diabetes (T2D) are frequently associated with nonalcoholic fatty liver disease (NAFLD), which in turn worsens the prognosis of T2D (1). Accumulation not only of triglycerides but even more of biologically active lipid intermediates, such as diacylglycerols and sphingolipids, has been frequently observed

[1]Division of Endocrinology and Diabetology, Medical Faculty, Heinrich-Heine University, Düsseldorf, Germany
[2]Institute for Clinical Diabetology, German Diabetes Center, Leibniz Center for Diabetes Research at Heinrich-Heine University, Düsseldorf, Germany
[3]German Center for Diabetes Research, München-Neuherberg, Germany
[4]Touchstone Diabetes Center, Department of Internal Medicine, The University of Texas Southwestern Medical Center, Dallas, TX
[5]Institute of Pathology, Medical Faculty, Heinrich-Heine University, Düsseldorf, Germany
[6]General Surgery Department, Schön Clinic, Düsseldorf, Germany

Corresponding author: Michael Roden, michael.roden@ddz.uni-duesseldorf.de.

Received 1 July 2017 and accepted 6 March 2018.

Clinical trial reg. no. NCT01477957, clinicaltrials.gov.

This article contains Supplementary Data online at http://care.diabetesjournals.org/lookup/suppl/doi:10.2337/dc17-1318/-/DC1.

in animal models of T2D and/or NAFLD. In rodent models, diacylglycerol and ceramide species were related to whole-body and hepatic insulin resistance and to ectopic lipid deposition, including hepatic steatosis (1,2). In humans, the role of circulating and tissue-specific concentrations of lipid intermediates for insulin resistance and ectopic lipid deposition is less clear. In skeletal muscle, specific diacylglycerol, but not ceramide, species predict the onset of insulin resistance (3). In the human liver, some studies reported a negative relationship between hepatic total diacylglycerols, but not ceramides, and insulin sensitivity (4–6) and an elevation of hepatic diacylglycerol concentrations in patients with NAFLD (7). Interestingly, recent data suggest that hepatic ceramide levels may dissociate liver steatosis from insulin resistance in NAFLD of different origin (8).

Patients at risk for or with overt T2D also frequently feature abnormal mitochondrial function linked to insulin resistance and NAFLD (9). Of note, obese people have increased hepatic mitochondrial capacity (10,11), which declines in nonalcoholic steatohepatitis (NASH) along with increased hepatic production of reactive oxygen species and oxidative DNA damage (10,12,13). Lactosylceramides have been implicated in the development of mitochondrial defects in the hearts of diabetic mice (14). In patients with coronary heart disease, plasma ceramides correlated not only with insulin resistance but also with systemic inflammation (15). Recent studies identified certain dihydroceramide species, particularly dihydroceramide 18:0, as biomarkers of diabetes onset in mice and humans (16). However, it remains unclear which pathways of sphingolipid metabolism are related to the adaptation of hepatic mitochondrial function and to oxidative stress and inflammation during progression of NAFLD, from steatosis or nonalcoholic fatty liver (NAFL) to NASH.

We thus aimed to examine the relationship of total and specific sphingolipid species in various tissues and in the circulation with hepatic and peripheral insulin sensitivity, hepatic mitochondrial function, oxidative stress, and inflammation in insulin-resistant people with NAFLD. To this end, we used comprehensive metabolic phenotyping to compare obese patients without steatosis (NAFL−) or with steatosis (NAFL+) or with NASH with healthy lean individuals serving as control (CON) undergoing bariatric or abdominal surgery.

RESEARCH DESIGN AND METHODS

Study Participants

The volunteers participated in a prospective study on obese humans undergoing bariatric surgery and on healthy humans undergoing elective abdominal surgery, such as cholecystectomy (n = 6) or herniotomy (n = 1), for nonmalignant diseases (clinical trial reg. no. NCT01477957, clinicaltrials.gov) (10). The current analysis comprised 21 obese (BMI $>$30 kg/m^2) patients and 7 CON subjects. The classification of obese patients into NAFL−, NAFL+, and NASH was based on liver histology using hematoxylin-eosin and special stainings (Van Gieson trichrome stain, Perls iron stain, periodic acid–Schiff–diastase, and Gomori reticulin stain), according to standard routine procedures, as previously described (10). NAFL+ was defined by the presence of $>$5% steatotic hepatocytes in a liver tissue section (17) and NASH by a NAFLD activity score of $\geq$5 (18). The NAFL+ group included one participant with T2D. All participants maintained stable body weight for at least 2 weeks before surgery. They gave written informed consent before inclusion in the study, which was approved by the Heinrich-Heine-University Düsseldorf Institutional Review Board and performed according to the World Medical Association Declaration of Helsinki.

Hyperinsulinemic-Euglycemic Clamp Test

The experimental procedures have been described in detail (1). Briefly, participants were asked to refrain from physical activity for 3 days before the clamp test. The patient with T2D withdrew oral glucose-lowering medication for 3 days before the test (19). On the day of the test and 1 week before surgery, participants arrived at the clinical research center at 0800 h, where they received two venous catheters in the antecubital veins of both arms for blood sampling and infusions of glucose and insulin. A primed-continuous infusion for 10 min (3.6 mg fasting glucose [mg/dL]/90 [mg/dL]/[min × kg body weight]) and infusion for 360 min (0.036 mg/[min × kg body weight]) of 98% enriched D-[6,6-$^2H_2$]glucose were performed until the end of the clamp test to measure endogenous glucose production (EGP). Insulin (Actrapid; Novo Nordisk) was administered as a primed-continuous infusion (40 mU/[m^2 body surface area × min]) from 0 to 180 min. Blood glucose measurements were performed every 5 min, and a 20% dextrose infusion labeled with D-[6,6-$^2H_2$]glucose (2% enriched) was adjusted to maintain normoglycemia (5 mmol/L). Whole-body insulin sensitivity was measured from whole-body mean glucose infusion rates (M value) with glucose space correction (19). The hepatic insulin sensitivity index (HIS) was calculated as the quotient of 100/(fasting EGP × fasting insulin concentration), and insulin-mediated EGP suppression was calculated as 100 × clamp EGP/fasting EGP (20).

Tissue Biopsies

Samples were obtained from the lower part of the right liver lobe, rectus abdominis muscle, the superficial layer of subcutaneous abdominal adipose tissue lying directly beneath the skin, and visceral abdominal adipose tissue surrounding intra-abdominal organs, respectively (amounts ranging between 200 and 1,000 mg). Serum samples for sphingolipids quantitation were also obtained during surgery. All specimens were taken by the surgeons at 30 min after induction of anesthesia according to standardized protocols (10). Aliquots of 100 mg fresh liver sample were fixed in 1% formaldehyde for histological examination, 50 mg was transferred into ice-cold biopsy preservation solution for high-resolution respirometry, and 200 mg was transferred into isolation buffer for isolation of mitochondria. Samples from liver and other tissues were all rapidly snap frozen in liquid nitrogen and stored at −80°C until further analysis.

Hepatic Oxidative Capacity

High-resolution respirometry was applied in liver tissue and—in case of sufficient amount of sample—also in isolated mitochondria upon exposure to various substrates for β-oxidation, tricarboxylic acid (TCA) cycle, and ADP titration, as previously described, after mechanical permeabilization of the liver sample (10,21). Mechanical permeabilization was performed to avoid potential cell damage and effects due to incubation with detergents. Because of the limited sample size of isolated mitochondria, we performed correlation analysis only for the liver tissue data. Of note, analysis of liver specimens yielding sufficient material for both

measurements of liver tissue and isolated mitochondria revealed a tight correlation of maximal uncoupled respiration between permeabilized tissue and isolated mitochondria (Supplementary Fig. 1). Maximal uncoupled (state u) respiration was measured after exposure to the mitochondrial uncoupler (carbonyl cyanide *p*-trifluoromethoxyphenylhydrazone) and adjusted for individual citrate synthase activity (CSA) and mitochondrial DNA as measures of mitochondrial content (10).

Hepatic Lipid Peroxidation and Systemic Inflammation

As a marker of lipid peroxidation, thiobarbituric acid–reactive substances (TBARS) were measured in serum and liver tissue as previously described (22). Catalase activity and 8-oxo-guanosine in hepatic tissue lysates were measured with ELISA (10). Interleukin 6 (IL-6), tumor necrosis factor-α (TNF-α) and IL-1 receptor antagonist (IL-1RA) were quantified using Quantikine HS (IL-6, TNF-α) or Quantikine (IL-1RA) ELISA kits (R&D Systems, Wiesbaden, Germany) (23). Total c-Jun N-terminal kinase (tJNK) and Thr183/Tyr185-phosphorylated (p)JNK were quantified using specific antibodies (Cell Signaling Technology) (10).

Laboratory Measurements

Blood glucose was measured with Cobas c311 (Roche Diagnostics, Mannheim, Germany), serum concentrations of insulin and C-peptide were measured with radioimmunoassay (Millipore, St. Charles, MI), and free fatty acids (FFAs) were measured microfluorometrically (24). Total adiponectin was measured in serum and plasma samples with the Human Adiponectin ELISA (Millipore).

Sphingolipid Measurements

Sphingolipids were quantified using liquid chromatography–tandem mass spectrometry (LC-MS/MS) methods (25). Briefly, flash-frozen tissue samples (40 mg) were homogenized in 2.0 mL organic extraction solvent (isopropanol:water:ethyl acetate, 25:10:65; volume [v]:v:v). Immediately afterward, 20 μL internal standard solution was added (AL Ceramide/Sphingoid Internal Standard Mixture II diluted 1:10 in ethanol; Avanti Polar Lipids, Alabaster, AL). The mixture was vortexed and sonicated in an ultrasonic bath for 40 min at 40°C. The samples were allowed to reach room temperature, and 1.5 mL high-performance LC (HPLC)–grade water was added. Two-phase liquid extraction was performed, the supernatant was transferred to a new tube, and the pellet was reextracted. Supernatants were combined and evaporated under nitrogen. The dried residue was reconstituted in 200 μL HPLC solvent B (methanol/formic acid 99:1; v:v, containing 5 mmol/L ammonium formate) for LC-MS/MS analysis. Lipid separation was achieved on a 2.1 (internal diameter) $\times$ 150 mm Kinetex C8, 2.6-μm core-shell particle column (Phenomenex, Torrance, CA). Plasma sphingolipids were quantified using a similar methodology requiring 50 μL serum. Sphingolipids were quantified using a Nexera X2 UHPLC system coupled to a Shimadzu LCMS-8050 triple quadrupole mass spectrometer operating the dual ion source in electrospray positive mode. Sphingolipid species were identified based on exact mass and fragmentation patterns and verified by lipid standards. The concentration of each metabolite was determined according to calibration curves using peak-to-area ratio of the analyte versus the corresponding internal standard. Calibration curves were generated using serial dilutions of each target analyte. Sphingolipid true standards were purchased from Avanti Polar Lipids.

Statistical Analysis

Data are presented as mean $\pm$ SD or median (25th, 75th percentiles) as appropriate. Differences in metabolic characteristics between the four groups of patients were calculated with ANOVA-like least-square linear regression using the Tukey-Kramer method to adjust for multiple comparisons of the four groups. Linear regression models were used to calculate *t* values (estimate/SEM) and *P* values of associations between metabolic parameters and sphingolipid species with and without adjustment for BMI. *P* values from two-sided tests $\leq$5% were considered to indicate significant differences. Analyses were performed using SAS version 9.4 software (SAS Institute, Cary, NC).

RESULTS

Participants' Characteristics

The groups had comparable age, sex, and levels of circulating triglycerides and FFAs (Table 1). BMI was similar across all obese groups (NAFL−, NAFL+, NASH) but was higher in all obese groups than in the CON group. HDL-cholesterol was higher in the CON group compared with NAFL− and NAFL+. LDL-cholesterol was higher in the NAFL− and NAFL+ groups than in the CON group. Peripheral insulin sensitivity was comparable in the three obese groups but markedly lower than in the CON group. Mean HIS was nominally higher in the CON group but not significantly different from that of the obese groups. The NAFLD score was higher in NAFL+ and NASH than in both NAFL− and CON. By definition of the groups, the level of hepatocellular lipids was similar in CON and NAFL− and lower than in NAFL+ and NASH, with NASH having more profound steatosis.

Tissue-Specific Sphingolipid Concentrations

We measured total ceramide species and dihydroceramides in serum and liver, which reflect de novo sphingolipid synthesis. Lactosylceramide and hexosylceramide species result from breakdown of more complex sphingolipids and therefore allow examining activation of the salvage pathway, which reuses these species. Figure 1 provides an overview of sphingolipid metabolism.

In serum, total ceramides were comparable, whereas total dihydroceramides were higher in NASH than in CON and NAFL− (Fig. 2*A* and *B*), a difference which remained significant after adjustment for BMI (*P* = 0.01 and 0.03, respectively). NASH had higher dihydroceramide species 16:0 compared with all other groups, species 22:0 compared with CON and NAFL−, and species 24:1 compared with CON (Fig. 2*C*). After BMI adjustment, dihydroceramides 22:0 and 24:1 were increased in NASH compared with CON (*P* = 0.01 for both) and NAFL− (dihydroceramide 22:0: *P* = 0.01; 24:1: *P* = 0.03).

Liver total ceramides were higher in NASH than in other groups (Fig. 2*D*). After adjustment for BMI, total ceramides were 33% and 50% higher in NASH compared with NAFL+ (*P* = 0.01) and NAFL− (*P* = 0.001). The increase in ceramide 16:0 in NAFL− compared with CON disappeared after adjustment for BMI. Independent of BMI, ceramide 24:0 was increased in NASH compared with all other groups ($P <$ 0.001). Overall, dihydroceramides and species 16:0, 22:0, and 24:1, as well as total lactosylceramides and species 24:1, were higher in NASH than in CON (Fig. 2*E* and *F*), only before adjustment for BMI. Hexosylceramides 22:0 and 24:0 were also increased in NASH (Fig. 2*E*), but only the

Table 1—Participant characteristics

	CON	NAFL−	NAFL+	NASH
N (females)	7 (5)	7 (6)	7 (4)	7 (6)
Age (years)	40 ± 13	43 ± 7	46 ± 12	42 ± 8
BMI (kg/m^2)	25.2 ± 3.3¶¶¶,###,***	49.5 ± 8.3	56.1 ± 7.0	51.4 ± 7.1
Waist circumference (cm)	82.8 ± 13.0¶¶,###,**	125.7 ± 19.8‡	144.5 ± 16.2	129.2 ± 17.0
Triglycerides (mg/dL)	75 (71, 94)	138 (74, 166)	135 (94, 286)	99.5 (94, 120)
FFA (μmol/L)	635 (473, 761)	819 (634, 947)	509 (261, 730)	599 (577, 671)
HDL-cholesterol (mg/dL)	64 (57, 83)¶,#	44 (35, 54)	35 (33,45)	52 (43, 59)
LDL-cholesterol (mg/dL)	89 (72, 99)¶,#	128 (105, 153)	128 (100, 151)	118 (107, 118)
Alanine aminotransferase (units/L)	25 (19, 34)	25 (14, 25)	22 (17, 25)	32 (28, 40)
Aspartate aminotransferase (units/L)	19 (19, 20)	20 (17, 23)	25 (19, 27)	25.5 (18, 31)
γ-Glutamyltransferase (units/L)	24 (16, 35)	16 (10, 35)	22 (15, 35)	32 (28, 40)
NAFLD activity score	0 (0, 2)##,***	0 (0, 1)‡‡,§§§	2 (2, 4)††	5 (4, 6)
Peripheral insulin sensitivity (mg/kg/min)	7.4 ± 2.2¶¶,##	3.1 ± 1.7	1.8 ± 0.3	2.8 ± 0.6
HIS index ([mg/kg/min]/[μU/mL])	15.1 ± 14.0	4.8 ± 2.1	1.7 ± 0.1	4.8 ± 4.4
Hepatocellular lipids (%)	1 (0, 5)##,***	2 (0, 5)‡‡,§§§	40 (10, 40)†	45 (40, 65)

Data are presented as mean ± SD or median (quartile 1, quartile 3) unless otherwise indicated **$P \leq 0.01$, ***$P < 0.001$ CON vs. NASH. ¶$P \leq 0.05$, ¶¶$P \leq 0.01$, ¶¶¶$P < 0.001$ CON vs. NAFL−. #$P \leq 0.05$, ##$P \leq 0.01$, ###$P < 0.001$ CON vs. NAFL+. ‡$P \leq 0.05$, ‡‡$P \leq 0.01$, NAFL− vs. NAFL+. §§§$P < 0.001$ NAFL− vs. NASH. †$P \leq 0.05$, ††$P \leq 0.01$ NAFL+ vs. NASH.

22:0 species remained increased compared with NAFL− and NAFL+ after BMI adjustment (P = 0.03 and 0.01, respectively).

Furthermore, we tested the associations of serum ceramides with the respective hepatic species to identify which possible circulating biomarkers reflect the progression of NAFLD. Relationships were found between certain serum and hepatic ceramide species. Serum concentrations of dihydroceramides (species 18:0, 20:0, 22:0, and 24:1) correlated positively with the respective hepatic concentrations (Supplementary Fig. 3*A*–*C*). Serum sphingomyelins 18:0, 24:0 (Supplementary Fig. 3*D*), and 18:1 also correlated positively with the respective hepatic sphingomyelin species.

Because sphingolipids can be derived from other tissues and have been implicated in their metabolism, we performed a comprehensive analysis of these metabolites in samples for skeletal muscle, visceral tissue, and subcutaneous tissue. In skeletal muscle, total ceramides were higher in NASH than in all other groups (Supplementary Fig. 2*A*). After BMI adjustment, NASH patients had still 26% and 24% higher ceramides than NAFL+ (P = 0.002) and NAFL− (P = 0.001), respectively. In subcutaneous and visceral adipose tissue, total ceramides were lower in NASH than in NAFL− and CON (Supplementary Fig. 2*B*). After BMI adjustment, NASH had 16% lower visceral adipose tissue ceramides than NAFL+ as well as 19% and 27% lower subcutaneous adipose tissue ceramides than NAFL+ (P = 0.04) and NAFL− (P = 0.003), respectively (Supplementary Fig. 2*C*). The complete data set of the various sphingolipids in all analyzed tissues is summarized in Supplementary Table 1.

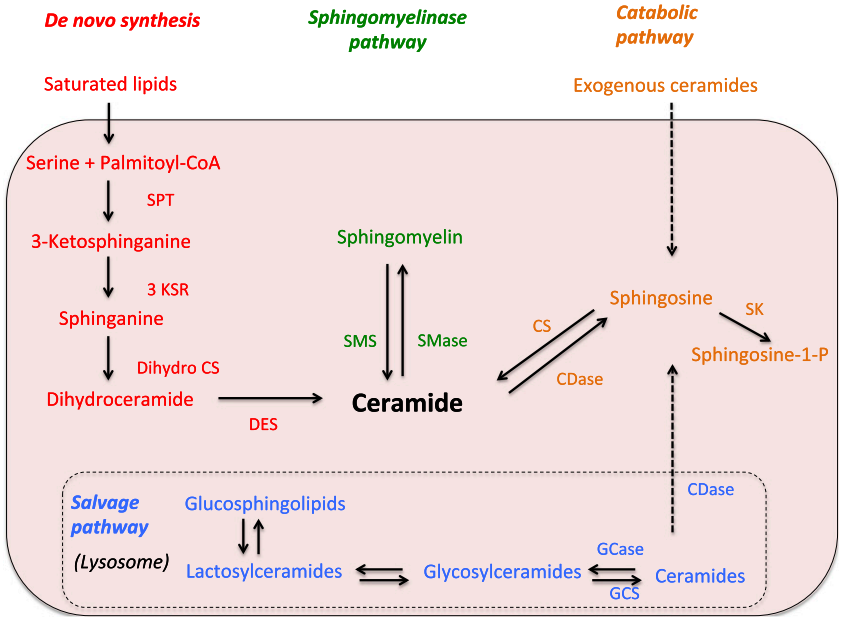

Figure 1—Overview figure of pathways involved in ceramide synthesis (de novo, sphingomyelinase, catabolic, salvage) and degradation to sphingosine and sphingosine-1-phosphate (P). CDase, ceramidase; CS, ceramide synthetase; DES, dihydroceramide desaturase; GCase, glycosylceramidase; GCS, glycosylceramide synthase; SK, sphingosine kinase; SMase, sphingomyelinase; SMS, sphingomyelin synthetase; SPT, serine palmitoyltransferase; 3 KSR, 3-ketosphinganine reductase.

Sphingolipids and Whole-Body and Hepatic Insulin Sensitivity

Due to the evidence for a role of sphingolipids in insulin resistance from rodent models, we also aimed at identifying relationships between sphingolipid species and peripheral and/or hepatic insulin sensitivity. We accounted for the overall body fat mass by testing these associations before and after adjustments for BMI. Serum ceramide species 16:0 (Fig. 3*A*), 18:0 (t = −2.2, P = 0.04), and 20:0 (t = −3.7, P = 0.001) correlated negatively with whole-body insulin sensitivity, as assessed by the M value. Total serum dihydroceramides (Fig. 3*B*) and

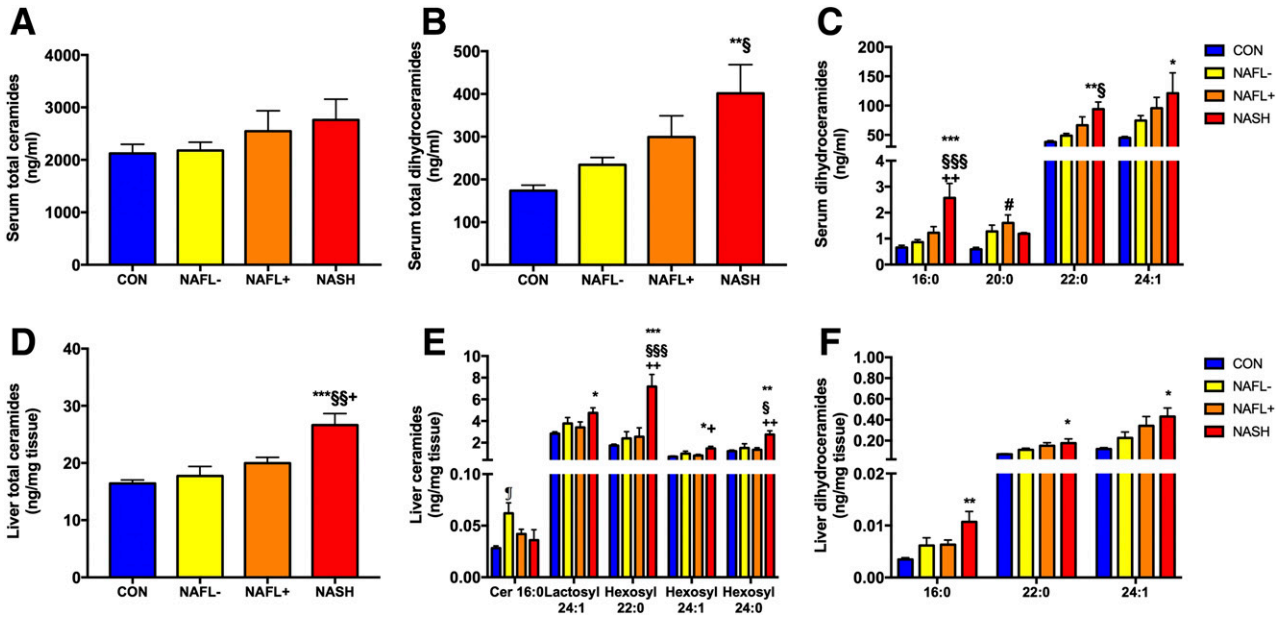

Figure 2—Total ceramides, dihydroceramides, and dihydroceramide species in serum (*A–C*) and liver (*D–F*) in lean individuals (CON) and obese NAFL− and NAFL+ participants and patients with NASH. Data are presented as mean ± SEM. Cer, ceramide; Hexosyl, hexoxylceramide; Lactosyl, lactosylceramide. ¶$P \leq 0.05$ CON vs. NAFL−. #$P \leq 0.05$ CON vs. NAFL+. *$P \leq 0.05$, **$P \leq 0.01$, ***$P < 0.001$ CON vs. NASH. §$P \leq 0.05$, §§$P \leq 0.01$, §§§$P < 0.001$ NAFL− vs. NASH. +$P \leq 0.05$, ++$P \leq 0.01$ NAFL+ vs. NASH.

dihydroceramide 20:0 ($t = -2.7$, $P = 0.01$) also correlated negatively with whole-body insulin sensitivity. In the liver, only dihydroceramides 22:0 ($t = -2.31$, $P = 0.04$) and 24:1 ($t = -2.3$, $P = 0.03$) correlated negatively with whole-body insulin sensitivity. Of note, these correlations disappeared after BMI adjustment. Deoxysphinganine in visceral and subcutaneous adipose tissue related negatively to whole-body insulin sensitivity (Fig. 3*C* and *D*), which remained only for the visceral adipose tissue compartment after BMI adjustment ($t = -2.51$, $P = 0.02$).

In serum, specific lactosylceramide species (18:0, 20:0, and 22:0) and hexosylceramide 18:0 related negatively with basal EGP ($t = -2.5$, $P = 0.03$; $t = -2.2$, $P = 0.04$; $t = -2.4$, $P = 0.03$; and $t = -3.1$, $P = 0.007$, respectively) after adjustment for BMI. Hepatic sphingosine related negatively with insulin-mediated EGP suppression ($t = -2.3$, $P = 0.03$).

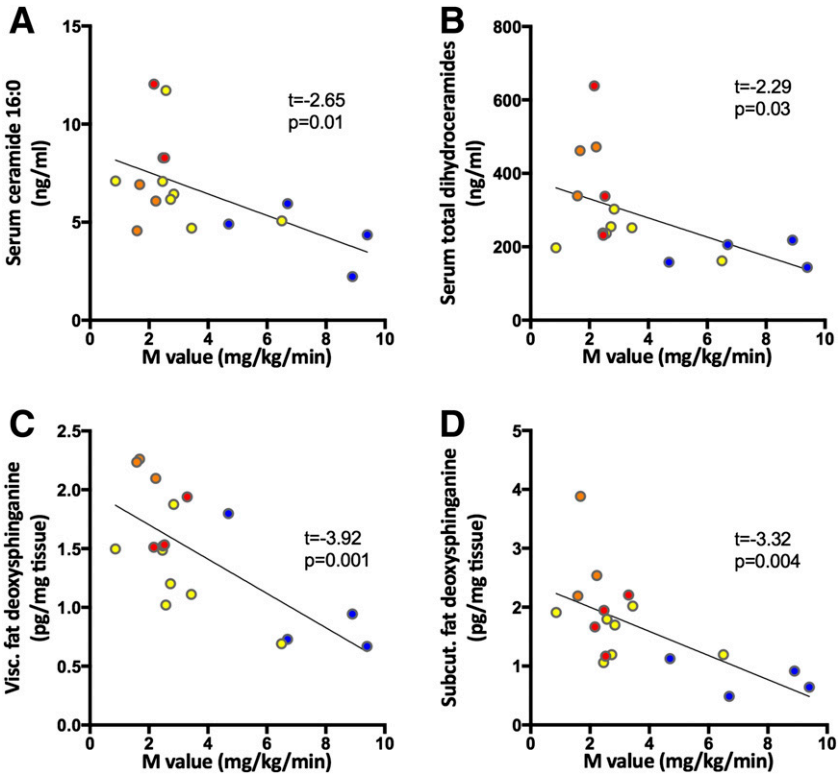

Figure 3—Correlations between ceramide species in serum (*A* and *B*), visceral (visc.) fat (*C*), and subcutaneous (subcut.) fat (*D*) and whole-body insulin sensitivity (M value) across all groups (CON: blue circles, NAFL−: yellow circles, NAFL+: orange circles, NASH: red circles).

Sphingolipids and Adiponectin Concentrations

Because of a possible interaction between sphingolipids with adiponectin and insulin resistance, we also examined the relationships of adiponectin with insulin sensitivity and ceramide levels in our cohort. Serum adiponectin correlated positively with whole-body insulin sensitivity (M value: $t = 3.14$, $P = 0.006$) and the HIS index ($t = 2.16$, $P = 0.01$). In visceral adipose tissue, total ceramides ($t = 6.42$, $P < 0.0001$) and lactosylceramide species 14:0, 16:0, 24:1, and 24:0 (all $t > 2.1$, $P < 0.04$) related positively to circulating adiponectin concentrations.

Sphingolipids and Hepatic Oxidative Capacity

Given the recently reported dynamic changes of mitochondrial function in

different stages of NAFLD, we tested associations of sphingolipid species with hepatic oxidative capacity and with a surrogate of mitochondrial density. Serum total lactosylceramides (Fig. 4*E*) and species 14:0 (t = 3.6, P = 0.001), 16:0 (t = 3.1, P = 0.007), and 24:1 (t = 2.3, P = 0.03) were associated with increased maximal uncoupled respiration from TCA cycle substrates after correction for CSA and adjustment for BMI. Hepatic sphinganine (t = 2.3, P = 0.03), sphingosine-1-phosphate (t = 2.17, P = 0.04), and lactosylceramide 14:0 (Fig. 4*F*) related positively to rates of state u respiration from TCA cycle substrates, after CSA correction and adjustment for BMI. Lactosylceramides 18:0 (t = 2.33, P = 0.03), 20:0 (t = 2.46, P = 0.02), and 14:0 (t = 2.97, P = 0.008) in serum and 22:0 (t = 2.42, P = 0.03) in the liver related to mitochondrial DNA content; however, these species did not associate with maximal respiration in the liver.

Hepatic Ceramide Species, Oxidative Stress, and Inflammation

The increase of sphingolipid species in NASH prompted us to further examine the relationship with markers of mechanisms involved in the pathogenesis of NASH, such as oxidative stress and inflammation. Liver TBARS correlated positively with liver total ceramides (Fig. 4*C*) and sphingomyelin 22:0. Further positive correlations of TBARS with hepatic ceramide 24:0 (Fig. 4*D*) and 24:1 disappeared after adjustment for BMI. Of note, hepatic ceramides did not relate to serum TBARS, hepatic catalase activity, and 8-oxo-guanosine (data not shown).

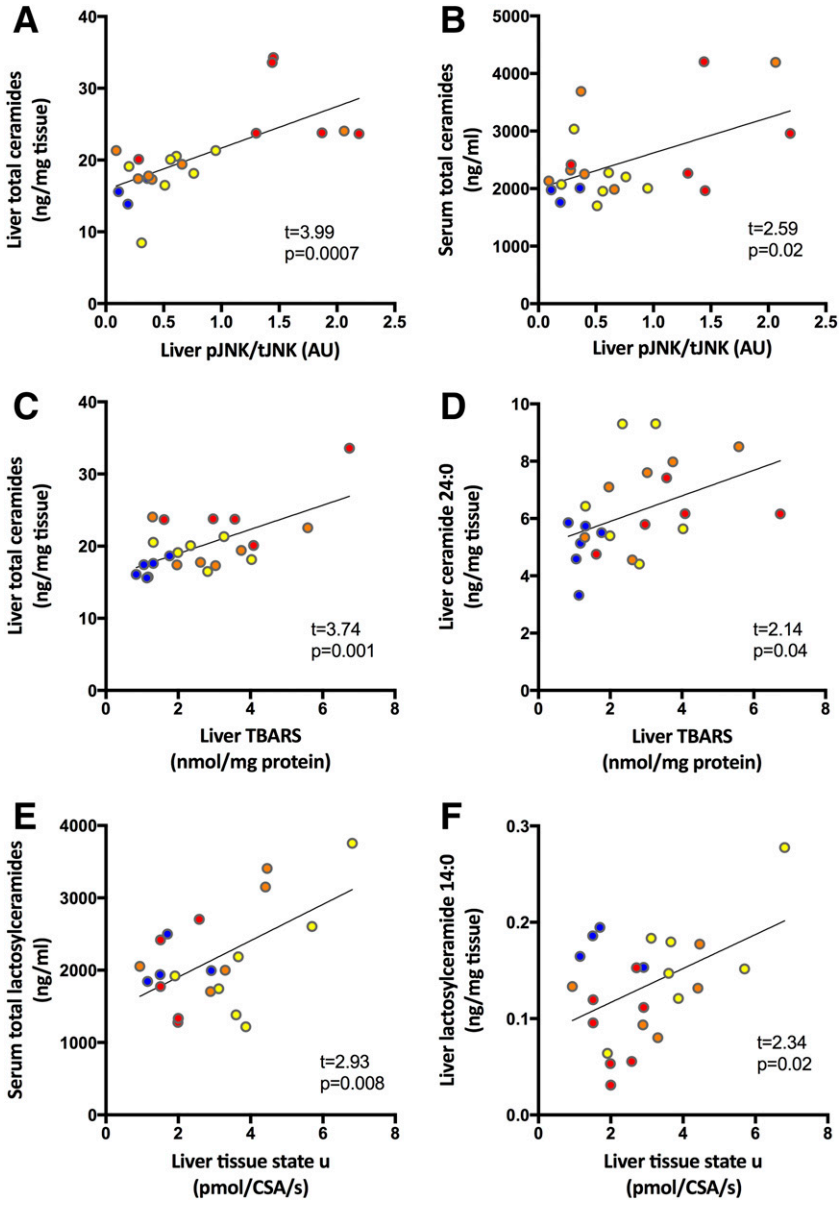

Figure 4—Correlations between liver Thr183/Tyr185–pJNK-to-tJNK ratio (*A* and *B*), TBARS in the liver (*C* and *D*), maximal uncoupled respiration (state u) of mitochondria in liver tissue corrected for CSA (*E* and *F*), and ceramide species in the liver (CON: blue circles, NAFL−: yellow circles, NAFL+: orange circles, NASH: red circles). AU, arbitrary units.

Overall, the hepatic pJNK-to-tJNK ratio correlated positively with serum and hepatic total ceramides (Fig. 4*A* and *B*) after adjustment for BMI. In serum, specific ceramide species 14:0 (t = 3.3, P = 0.003), 16:0 (t = 2.5, P = 0.02), 18:0 (t = 2.6, P = 0.01), and 24:0 (t = 2.7, P = 0.01), dihydroceramides species 16:0 (t = 4.8, P = 0.0001) and 22:0 (t = 4.1, P = 0.0006), hexosylceramide species 22:0 (t = 3.5, P = 0.002), and lactosylceramide species 24:0 (t = 3.1, P = 0.006) all correlated positively with the pJNK-to-tJNK ratio after BMI adjustment. In the liver, ceramide 24:0 and hexosylceramides 22:0 (t = 5.2, $P <$ 0.0001), 24:0 (t = 3.1, P = 0.006), and 24:1 (t = 2.4, P = 0.02) also related to increased pJNK-to-tJNK ratio. The positive associations of liver pJNK with hepatic total lactosylceramides and its species 16:0 and 24:1 were abolished after adjustment for BMI.

We performed additional exploratory linear regression analyses within the four patient groups to identify possible differences between the obese patients with or without NASH. Lactosylceramide 14:0 in serum (CON: t = −0.14, P = 0.88; NAFL−: t = 2.42, P = 0.03; NAFL+: t = 2.35, P = 0.03; NASH: t = −0.87, P = 0.39), serum total lactosylceramides (CON: t = 0.07, P = 0.94; NAFL−: t = 2.71, P = 0.01; NAFL+: t = 1.81, P = 0.09; NASH: t = 0.52, P = 0.60), hepatic sphinganine, and hepatic lactosylceramide 14:0 (Supplementary Table 2) showed increased slopes in the obese NAFL− group and decreased or even inverse slopes within the NASH group. Furthermore, we found greater slopes and significant correlations of liver total ceramides with TBARS in the NASH group (Supplementary Table 2).

In addition, we assessed the role of sphingolipids not only for hepatic but also for circulating markers of inflammation. Although we found some correlations of serum ceramide species 14:0 (t = 2.75, P = 0.01) and serum sphingosine (t = 2.70, P = 0.01) with circulating TNF-α

concentrations even after adjustment for BMI, neither serum nor hepatic sphingolipids correlated with circulating IL-6 levels (data not shown).

CONCLUSIONS

The main findings of this study are that *1*) insulin-resistant patients with NASH exhibit higher hepatic concentrations of total ceramides, certain dihydroceramides, and lactosylceramides, *2*) hepatic dihydroceramide species 22:0 and 24:1 correlate negatively with whole-body insulin sensitivity, *3*) total hepatic dihydroceramides and species and hexosylceramides and lactosylceramides associate with hepatic oxidative stress and activation of hepatic inflammatory pathways, and *4*) higher lipid peroxidation along with lower hepatic mitochondrial respiration relates to increased hepatic ceramides in obese patients with NASH.

Rodent studies using a high-fat diet or in leptin-deficient *ob*/*ob* mice have shown controversial results for the relationship of hepatic accumulation of ceramides with hepatic insulin sensitivity (26,27). Here we report that obese patients with NASH have elevated liver total ceramides, dihydroceramides, and lactosylceramides, even after adjustment for BMI. Furthermore, specific ceramide species (i.e., serum dihydroceramides 22:0 and 24:1 as well as hepatic ceramide 24:0) are characteristic for the presence of NASH, whereas other species were already elevated in obesity without NAFLD. This extends findings showing higher liver total ceramides and dihydroceramides in insulin-resistant people (8). In the current study, hepatic ceramide species did not correlate with basal EGP, whereas hepatic sphingosine related negatively with hepatic insulin sensitivity. Hepatic insulin sensitivity also did not correlate with liver total ceramides among obese patients in previous studies (4). More recently, hepatic insulin sensitivity was related to cytosolic diacylglycerol but not to total hepatic ceramides (6).

We found that serum ceramide species 16:0, 18:0, and 20:0 and total and dihydroceramide species 20:0 showed inverse associations with whole-body insulin sensitivity, as assessed with the gold standard clamp technique, but not after adjustment for BMI. This suggests that the observed correlations with M value were mediated solely by obesity. Increased dihydroceramide species reflect activation of de novo ceramide synthetic pathway, resulting from condensation of palmitoyl-CoA with serine and mediated by serine palmitoyltransferase. Targeted inhibition of this enzyme in mice showed reversal of glucose intolerance and whole-body insulin resistance in diet-induced obesity (28). Hepatic dihydroceramides 22:0 and 24:0 correlated negatively with the M value, in line with findings in insulin-resistant patients, underlining the role of de novo ceramide synthesis in human NAFLD (8). Liver total ceramides did not relate to whole-body insulin sensitivity, extending previous findings using HOMA-insulin resistance as a surrogate of insulin resistance (5). Similarly, total ceramides were also elevated in skeletal muscle of NASH patients, in line with studies in severe obesity (29,30), but did not relate to peripheral insulin resistance.

Serum total lactosylceramides and subspecies, as well as hepatic sphinganine and sphingosine-1-phosphate, correlated with increased maximal uncoupled respiration of hepatic mitochondria. Of note, increased lipid oxidation and oxidative capacity has been identified as an important mechanism contributing to the progression of NAFLD in obese patients (10,11). Hepatic ceramides, diacylglycerols, and acylcarnitines have been previously found increased, along with induced TCA cycle, in mice with NASH (31). Lipid oversupply with subsequent high rates of lipid oxidation leads to oxidative stress and damage of the respiratory chain, resulting in decreased ATP production (20) and insulin resistance (9).

Hepatic total ceramides and sphingomyelin 22:0 associated positively with hepatic lipid peroxidation as assessed from TBARS. Ceramides have been suggested to induce reactive oxygen species production with subsequent opening of the mitochondrial permeability pore and cytochrome c release in isolated mitochondria of rat liver (32). More recently, lactosylceramides have been indicated as mediators of oxidative stress by inhibition of the respiratory chain and increased sensitivity of the mitochondrial permeability transition pore to Ca^{2+} in heart mitochondria of diabetic mice (14). Lactosylceramides and hexosylceramides originate from degradation of more complex glycosphingolipids in lysosomes and can be further reused in the "salvage pathway" for ceramide synthesis. Thus, the increase in these species could reflect secondary changes occurring with obesity-associated NAFLD. Importantly, we found that the NASH group featured decreased hepatic mitochondrial respiration along with increased lipid peroxidation, which in turn correlated with hepatic ceramides. This extends our previous findings on the lost adaptation of hepatic mitochondria due to increased oxidative stress in NASH livers (10).

Increased adiponectin has been shown to play a central role in NASH by improving liver histology in response to pioglitazone treatment (33) and to be associated with reduced tissue ceramides (29,30). Most recently, adiponectin receptors were attributed to have an inherent ceramidase activity, hydrolyzing ceramides to sphingosine and FFA, which may be a novel mechanism underlying the beneficial metabolic effects of adiponectin (34). The current study confirmed that serum adiponectin levels relate to improved hepatic and peripheral insulin sensitivity but did not detect associations with hepatic or circulating ceramides. However, total ceramides and certain lactosylceramides in visceral adipose tissue positively related to serum adiponectin levels, likely reflecting the increased total ceramide levels in visceral adipose tissue among lean, insulin-sensitive individuals compared with obese individuals.

Increasing hepatic ceramides and ceramide 24:0, as well as hexosylceramide species 22:0, 24:0, and 24:1, paralleled raising hepatic inflammation as assessed from the hepatic pJNK-to-tJNK ratio. Activation of TLR4 by saturated fatty acids leads to transcriptional activation of ceramide synthases and subsequently to ceramide elevation, inhibition of Akt, and insulin resistance (35). In the current study, circulating TNF-α levels also correlated with ceramide 14:0 and sphingosine, indicating that sphingolipids relate not only to intrahepatic but also to systemic inflammation in NAFLD. Of note, one previous study reported similar associations with the ceramides 18:0 and 18:1 in patients with overt T2D (36).

Finally, this study comprehensively analyzed sphingolipid levels in multiple tissues, which allowed us to identify that ceramide subsets, specifically, and species as well as certain sphingomyelins in serum reflect the respective species in the liver. Plasma dihydroceramide species and, specifically, 18:0 were also recently identified as markers for diabetes development

in the following 9 years (16). In the current study, serum dihydroceramide 18:0 correlated with the respective concentrations in the liver. The present finding might therefore be helpful for the future use of certain serum sphingolipids as biomarkers for the detection and progression of NAFLD as well as a link between NAFLD and diabetes onset.

Strengths of our study are the simultaneous analysis of biopsy samples obtained from various tissues relevant to whole-body and hepatic metabolism from obese patients with and without steatosis and NASH but also from healthy lean volunteers. All participants were thoroughly phenotyped using gold-standard techniques. Insulin sensitivity, mitochondrial function, lipid peroxidation, and inflammation were all also measured at the hepatic level.

The main limitation resides in the cross-sectional study design, which does not allow conclusions about the causality of the observed associations. Six of seven of our lean CON subjects underwent cholecystectomy. However, although increased ceramide concentrations in serum and in bile have been reported in mice fed a lithogenic diet (37), whether cholecystectomy affects sphingolipid metabolism in healthy, lean humans is unknown.

In conclusion, several sphingolipids are elevated in insulin-resistant people with NASH, and certain hepatic sphingolipids, such as dihydroceramides and lactosylceramides, specifically relate to hepatic oxidative stress and inflammation, suggesting that these lipid metabolites contribute to the progression of simple fatty liver to NASH in humans. These findings further imply different contributions of de novo ceramide synthesis and the salvage pathway for peripheral insulin resistance and hepatic oxidative stress/inflammation, respectively. They further highlight the importance of focusing on specific sphingolipid subspecies rather than on total levels of the different ceramides and sphingosines when analyzing their role for hepatic inflammation and abnormal mitochondrial function.

Acknowledgments. The authors thank Dr. Julia Szendroedi for her contribution to the clinical experiments and Kai Tinnes, Myrko Esser, and Ulrike Partke (all from the Institute for Clinical Diabetology, German Diabetes Center, Leibniz Center for Diabetes Research at Heinrich-Heine University, Düsseldorf, Germany) for their excellent technical support.

Funding. This study was supported in part by the Ministry of Science and Research of the State of North Rhine-Westfalia and the German Federal Ministry of Health (BMG); by a grant from the Federal Ministry for Research (BMBF) to the German Center for Diabetes Research (DZD Grant 2012); by grants from the Helmholtz portfolio theme "Metabolic Dysfunction and Common Disease," the Helmholtz Alliance to Universities "Imaging and Curing Environmental Metabolic Diseases (ICEMED)," the German Research Foundation (SFB 1116), the German Diabetes Association, and the Schmutzler Stiftung; and by funding from the Touchstone Diabetes Center at the University of Texas Southwestern Medical Center (to P.E.S.).

Duality of Interest. No potential conflicts of interest relevant to this article were reported.

Author Contributions. M.A. and R.G. obtained and analyzed the data and wrote, edited, and reviewed the manuscript. C.K. and S.G. performed the clinical experiments and edited and reviewed the manuscript. T.J., E.D.F., C.H., D.M., F.J., and I.E. performed laboratory analyses and edited and reviewed the manuscript. M.S. obtained tissue samples during surgery and edited and reviewed the manuscript. P.E.S. led the sphingolipid measurements and wrote, reviewed, and edited the manuscript. M.R. initiated the investigation, designed and led the clinical experiments, and wrote, reviewed, and edited the manuscript. All authors gave final approval of the version to be published. M.R. is the guarantor of this work and, as such, had full access to all the data in the study and takes responsibility for the integrity of the data and the accuracy of the data analysis.

Prior Presentation. Parts of this study were presented in abstract form at the 77th Scientific Sessions of the American Diabetes Association, San Diego, CA, 9–13 June 2017.

References

1. Tilg H, Moschen AR, Roden M. NAFLD and diabetes mellitus. Nat Rev Gastroenterol Hepatol 2017;14:32–42
2. Chaurasia B, Summers SA. Ceramides—lipotoxic inducers of metabolic disorders [published correction appears in Trends Endocrinol Metab 2018;29:66–67]. Trends Endocrinol Metab 2015;26:538–550
3. Szendroedi J, Yoshimura T, Phielix E, et al. Role of diacylglycerol activation of PKCθ in lipid-induced muscle insulin resistance in humans. Proc Natl Acad Sci U S A 2014;111:9597–9602
4. Magkos F, Su X, Bradley D, et al. Intrahepatic diacylglycerol content is associated with hepatic insulin resistance in obese subjects. Gastroenterology 2012;142:1444–1446.e1442
5. Kumashiro N, Erion DM, Zhang D, et al. Cellular mechanism of insulin resistance in nonalcoholic fatty liver disease. Proc Natl Acad Sci U S A 2011;108:16381–16385
6. Ter Horst KW, Gilijamse PW, Versteeg RI, et al. Hepatic diacylglycerol-associated protein kinase Cε translocation links hepatic steatosis to hepatic insulin resistance in humans. Cell Reports 2017;19:1997–2004
7. Kotronen A, Seppänen-Laakso T, Westerbacka J, et al. Hepatic stearoyl-CoA desaturase (SCD)-1 activity and diacylglycerol but not ceramide concentrations are increased in the nonalcoholic human fatty liver. Diabetes 2009;58:203–208
8. Luukkonen PK, Zhou Y, Sädevirta S, et al. Hepatic ceramides dissociate steatosis and insulin resistance in patients with non-alcoholic fatty liver disease. J Hepatol 2016;64:1167–1175
9. Szendroedi J, Phielix E, Roden M. The role of mitochondria in insulin resistance and type 2 diabetes mellitus. Nat Rev Endocrinol 2011;8:92–103
10. Koliaki C, Szendroedi J, Kaul K, et al. Adaptation of hepatic mitochondrial function in humans with non-alcoholic fatty liver is lost in steatohepatitis. Cell Metab 2015;21:739–746
11. Sunny NE, Parks EJ, Browning JD, Burgess SC. Excessive hepatic mitochondrial TCA cycle and gluconeogenesis in humans with nonalcoholic fatty liver disease. Cell Metab 2011;14:804–810
12. Gornicka A, Morris-Stiff G, Thapaliya S, Papouchado BG, Berk M, Feldstein AE. Transcriptional profile of genes involved in oxidative stress and antioxidant defense in a dietary murine model of steatohepatitis. Antioxid Redox Signal 2011;15:437–445
13. Seki S, Kitada T, Yamada T, Sakaguchi H, Nakatani K, Wakasa K. In situ detection of lipid peroxidation and oxidative DNA damage in non-alcoholic fatty liver diseases. J Hepatol 2002;37:56–62
14. Novgorodov SA, Riley CL, Yu J, et al. Lactosylceramide contributes to mitochondrial dysfunction in diabetes. J Lipid Res 2016;57:546–562
15. de Mello VD, Lankinen M, Schwab U, et al. Link between plasma ceramides, inflammation and insulin resistance: association with serum IL-6 concentration in patients with coronary heart disease. Diabetologia 2009;52:2612–2615
16. Wigger L, Cruciani-Guglielmacci C, Nicolas A, et al. Plasma dihydroceramides are diabetes susceptibility biomarker candidates in mice and humans. Cell Reports 2017;18:2269–2279
17. Brunt EM, Tiniakos DG. Histopathology of nonalcoholic fatty liver disease. World J Gastroenterol 2010;16:5286–5296
18. Kleiner DE, Brunt EM, Van Natta M, et al.; Nonalcoholic Steatohepatitis Clinical Research Network. Design and validation of a histological scoring system for nonalcoholic fatty liver disease. Hepatology 2005;41:1313–1321
19. Apostolopoulou M, Strassburger K, Herder C, et al.; GDS group. Metabolic flexibility and oxidative capacity independently associate with insulin sensitivity in individuals with newly diagnosed type 2 diabetes. Diabetologia 2016;59:2203–2207
20. Szendroedi J, Chmelik M, Schmid AI, et al. Abnormal hepatic energy homeostasis in type 2 diabetes. Hepatology 2009;50:1079–1086
21. Kuznetsov AV, Kehrer I, Kozlov AV, et al. Mitochondrial ROS production under cellular stress: comparison of different detection methods. Anal Bioanal Chem 2011;400:2383–2390
22. Jelenik T, Séquaris G, Kaul K, et al. Tissue-specific differences in the development of insulin resistance in a mouse model for type 1 diabetes. Diabetes 2014;63:3856–3867
23. Herder C, Bongaerts BWC, Rathmann W, et al. Association of subclinical inflammation with polyneuropathy in the older population: KORA F4 study. Diabetes Care 2013;36:3663–3670
24. Szendroedi J, Saxena A, Weber KS, et al.; GDS Group. Cohort profile: the German Diabetes Study (GDS). Cardiovasc Diabetol 2016;15:59
25. Holland WL, Adams AC, Brozinick JT, et al. An FGF21-adiponectin-ceramide axis controls energy

expenditure and insulin action in mice. Cell Metab 2013;17:790–797
26. Holland WL, Miller RA, Wang ZV, et al. Receptor-mediated activation of ceramidase activity initiates the pleiotropic actions of adiponectin. Nat Med 2011;17:55–63
27. Trevino MB, Mazur-Hart D, Machida Y, et al. Liver perilipin 5 expression worsens hepatosteatosis but not insulin resistance in high fat-fed mice. Mol Endocrinol 2015;29:1414–1425
28. Ussher JR, Koves TR, Cadete VJ, et al. Inhibition of de novo ceramide synthesis reverses diet-induced insulin resistance and enhances whole-body oxygen consumption. Diabetes 2010;59:2453–2464
29. Xia JY, Morley TS, Scherer PE. The adipokine/ceramide axis: key aspects of insulin sensitization. Biochimie 2014;96:130–139
30. Warshauer JT, Lopez X, Gordillo R, et al. Effect of pioglitazone on plasma ceramides in adults with metabolic syndrome. Diabetes Metab Res Rev 2015;31:734–744
31. Patterson RE, Kalavalapalli S, Williams CM, et al. Lipotoxicity in steatohepatitis occurs despite an increase in tricarboxylic acid cycle activity. Am J Physiol Endocrinol Metab 2016;310:E484–E494
32. García-Ruiz C, Colell A, París R, Fernández-Checa JC. Direct interaction of GD3 ganglioside with mitochondria generates reactive oxygen species followed by mitochondrial permeability transition, cytochrome c release, and caspase activation. FASEB J 2000;14:847–858
33. Gastaldelli A, Harrison S, Belfort-Aguiar R, et al. Pioglitazone in the treatment of NASH: the role of adiponectin. Aliment Pharmacol Ther 2010;32:769–775
34. Holland WL, Scherer PE. Structural biology: receptors grease the metabolic wheels. Nature 2017;544:42–44
35. Maceyka M, Spiegel S. Sphingolipid metabolites in inflammatory disease. Nature 2014;510:58–67
36. Haus JM, Kashyap SR, Kasumov T, et al. Plasma ceramides are elevated in obese subjects with type 2 diabetes and correlate with the severity of insulin resistance. Diabetes 2009;58:337–343
37. Lee BJ, Kim JS, Kim BK, et al. Effects of sphingolipid synthesis inhibition on cholesterol gallstone formation in C57BL/6J mice. J Gastroenterol Hepatol 2010;25:1105–1110